International Journal of Engineering and Modern Technology E-ISSN 2504-8848 P-ISSN 2695-2149
Vol. 6 No. 2 2020 www.iiardpub.org

3D Multiphase Flow Compositional Modeling of Pressure Distribution for Niger – Delta Gas Condensate Reservoirs; (A Numerical Approach)

[1]Pepple Daniel Dasigha, [2]Nmegbu Chukwuma Godwin J. & [3]Ehirim Emmanuel O.
[1,2](Department of Petroleum Engineering, Rivers State University, Port-Harcourt, Nigeria).
[3](Department of Chemical/Petrochemical Engineering, Rivers State University, Port-Harcourt, Nigeria).

[1]dasigha.pepple@ust.edu.ng [2]nmegbu.godwin@ust.edu.ng [3]ehirim.emmanuel@ust.edu.ng

Abstract
Pressure transient analysis and pressure distribution equations for gas condensate reservoirs have constantly been reviewed over time. This is because several isothermal depletion processes for these extremely pressure-sensitive reservoir systems are not only dependent on production rates but also a function of lithology and reservoir rock orientation. This translates that additional pressure drawdowns traditionally influenced by lithology, if not accurately accounted for may potentially truncate reservoir performance predictions, particularly for a skin–prone Niger Delta sandstone formation. In this study, a 3D multi-phase flow compositional model that integrates a non–Darcy turbulent flow coefficient and the lithology factor for a Niger Delta sandstone formation was developed. Subroutines for model resolution involved a relative permeability analysis and an adequate reservoir fluid characterization via PVT modeling. This approach revealed that the 13-component mixture was characterized as a dew point system with a saturation pressure of 3825.86 psia. Other PVT modeling deductions revealed a GOR of 5541 scf/STB, CGR of 180.47 STB/MMscf, oil gravity of 74.84^{O}API, critical temperature of 219.1 ^{O}F, cricondenterm of 422.1 ^{O}F, gas viscosity of 0.048cp and formation volume factor of 0.003771 cf/scf at initial conditions of pressure and temperature of 4991.70psia and 221.0^{O}F respectively. These parameters when substituted into the derived characteristic equation yield a series of constants required for the model resolution. Having a maximum iterative convergence error of 0.01%, the discretized 20 pressure unknowns which was linearized from their partial differential equivalent was resolved by adopting the Successive-Over-Relaxation technique with ω_{opt}=1.3. The validity of the deduced characteristic equation was established upon matching it with a conventional 3D pressure distribution model and results when compared showed that for the deduced model, an additional pressure drop of 34.25 psi in the production grid block after 15days is inevitable due to consideration of the unconsolidated nature of the sandstone reservoir for which the conventional 3D model tends to ignore.

Keywords: *Gas Condensate, Modeling, Niger Delta, Pressure Distribution, Sandstone, Skin, Successive Over Relaxation*

I. INTRODUCTION

One of the basic cruxes of engineering in Nigeria is to harness the energy of the region in its potent form to meet certain energy demands. Most often than not in the process, energy is converted from its natural form into one which must be highly palatable with human utilization. Petroleum and Natural Gas Engineering isn't any different. It is focused on successfully extracting petroleum buried deep in the subsurface and getting it to where it is needed. The petroleum fluids of particular interest to the Petroleum and Gas engineers are crude oil and natural gases.

Nigeria has an estimated proven natural gas reserve of about 180 trillion cu-ft, making it the largest in Africa and ranking ninth in the world with a 50 – 50 estimated distribution ratios between Non-Associated Gas (NAG) and Associated Gas (AG) (The World Factbook, 2017). Gas condensate reservoirs often found as a single-phase gas at the time of discovery are encountered more frequently as exploration is now targeted at deeper zones, higher pressures and elevated temperatures (Wilson, 2003; Abekah, 2016; Rousennac, 2001).
In reservoir engineering, describing a typical gas condensate reservoir can be done with the traditional P-T or phase diagram. These reservoirs are essential sources of hydrocarbon reserves and have been renowned as that which possesses complicated flow behavior and dynamics, characterized by producing both liquid condensates and gases at the surface. During the exploitation of these distinct reservoirs, the initial reservoir pressure drops as the fluid moves towards the producing well. When pressure drops below the dew point of the gas condensate reservoir, the liquid starts to drop out of the gas. This phenomenon is known as retrograde condensation (khanal, 2014; Mindek, 2005).
As a reservoir produces, formation temperature usually does not change, but the pressure decreases. When the pressure in a gas-condensate reservoir decreases to a certain point called the saturation pressure or dew-point pressure, a liquid phase rich in heavy ends drops out of solution; the gas phase is slightly depleted of its heavy ends. A continued decrease in pressure increases the volume of the liquid phase up to a maximum amount; liquid volume then seizes to increase further. This behavior can be displayed in a pressure-volume-temperature (PVT) diagram for gas condensate reservoir. The amount of liquid phase present depends not only on the pressure and temperature but also on the composition of the fluid. A dry gas by definition has insufficient heavy components to generate liquids in the reservoir even with near wellbore drawdown conditions (Vo, 2010; Gunderson, 2013).
Most authors have argued that the engineering of a gas condensate field is 80% traditional "gas" engineering and 20% "extra" engineering. The numbers could be 90 – 10 or 70 – 30, but the majority of engineering of any gas condensate field is always the same as the engineering of a gas reservoir without condensate. The major distinction between a gas condensate field and that of a "dry" gas is typically the extra valuable proceeds derived from surface condensate production. The production of these condensates evolves from the produced reservoir gas to the produced "wet gas" and then the produced well stream which is processed at the surface (Whitson *et al.*, 1999).

The production rate for these systems is not only a function of pressure gradient but also as a result of complexities dependent on the flowing bottom hole pressure (FBHP). The FBHP to a large extent determines the distribution of condensate accumulation around the wellbore vicinity. The formation of a retrograde condensates results in a buildup of a liquid phase around the wellbore, leading to a decrease in the effective permeability to gas into the wellbore. The liquid dropout first occurs near the wellbore and propagates radially away from the well (assuming the well at the center of a radial reservoir) (Lal, 2003). According to Rousennac, (2001), after retrograde condensation occurs when reservoir pressure around a well drops below the dew-point pressure, three regions are created with different liquid saturations. Further away from the well, an outer region which has the initial liquid and gas saturations; next, there is an intermediate region with a rapidly increasing liquid saturation and a corresponding decrease in gas relative permeability. Liquids in that region are less than the critical condensate saturation and hence, immobile. Closer to the well, an inner region forms where the liquid saturation reaches a critical value and the effluent travels as two-phase flow with a constant composition (the condensate deposited as pressure decreases is equal to that flowing towards the well). There may also exist a fourth region near the well where low interfacial tensions (IFT) at high rates yield a decrease in liquid saturation and an increase in gas relative permeability (Lal, 2003; Roussennac, 2001).

Characterization of gas condensate reservoirs is a difficult task, since multiphase flow in the reservoir, phase alterations, and in some cases, changes of the mixture composition during flow towards the well largely complicates well test interpretations. Gas condensate – related areas such as well deliverability, well test interpretation and reservoir flow dynamics in general, have been long-standing problems for previous researchers. Most well test evaluation for reservoir characterization in a dynamic system strongly depends on the pressure transient response or the pressure distribution in both spatial (radial distance or x,y,z coordinates) and time domains across the reservoir. Drawdowns are not only influenced by production rates but also by the geologic configuration for the reservoir rock (particularly the Niger Delta sandstone formation which is characterized as being well sorted but highly unconsolidated and prone to fines migration). Hence an erroneous reservoir pressure distribution prediction as a result of the negligence of reservoir rock type is capable of incurring early abandonment, particularly for a pressure-sensitive system like gas condensate reservoirs where retrograde condensation can occur and impair flow within the slightest drop in pressure below the saturation pressure. This study is therefore aimed at developing a multi-dimensional flow compositional pressure predictor expression that can accurately simulate the performance prediction of gas condensate reservoirs in the Niger-Delta.

II. RESEARCH METHODOLOGY

2.1 Fundamental Principles and Reservoir Description

The fundamental principles upon which the predictor model is developed include; Material balance account (law of mass conservation), Equations of State, Darcy law, multiphase relative permeability concept, reservoir geometry assumptions and porous media fluid transport equations. The reservoir of interest is a 103 ft (31.39 m) thick gas condensate reservoir buried 11,782 ft (238.35 m) to HWC from a sea bed of 315 ft (96.01 m) water depth in an offshore field within the Niger Delta. Reservoir rock description reveals an unconsolidated sandstone formation with an average porosity of 22.11% and an average formation absolute permeability of 192.07mD. Fluid characterization reveals an initial gas saturation of 77.89% with minimal traces of sour components (CO_2, H_2S, N_2 Etc).

2.2 Simulators Used

The simulators for this study were limited to Petroleum Expert's *PVTp*, Microsoft Excel VBA, and Matlab R2007a. The Excel VBA simulator proved a useful tool in the determination and simulation of certain desired unknowns across discrete points of the gas condensate reservoir system. The *PVTp* simulator which is integral to the IPM (Integrated Production Management) suite was used to accurately characterize the reservoir in terms of reservoir critical properties. It also was instrumental in generating PVT properties of the gas condensate fluid system used for performance prediction modeling. Having deduced PVT parameters, the program code for the characteristic equations which integrates PVT properties was written using Matlab R2007a with initial and boundary conditions properly defined. To attain an accelerated parameter convergence, the iterative solver of Microsoft Excel VBA 2013 proved useful in the stepwise updates of deduced reservoir parameters and played an important role in the implementation of the iterative relaxation function.

2.3 Model Development

Consider a control volume of the representative block of a porous medium with mass entry and mass exit at points A, C and E to B, D and F respectively in the figure below. For a material balance account, we can recall the law of conservation of mass, stated as follows;

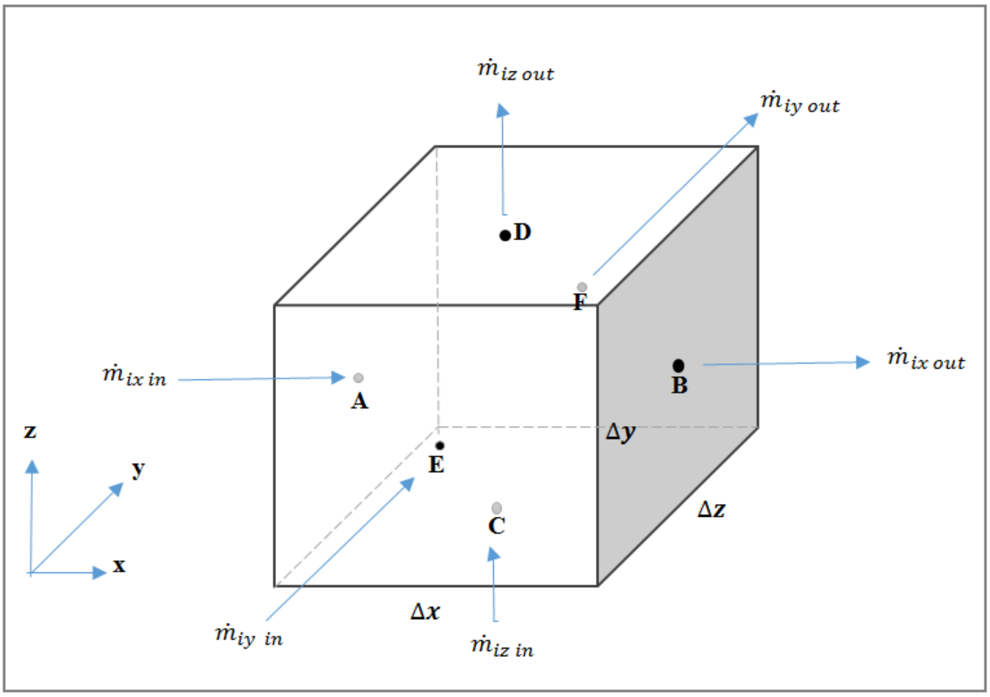

Figure 1: Representative Control Volume of a Porous Medium

Mass of Component *i* at Entry – Mass of Component *i* at Exit + Net Mass Generation/Depletion of *i* Component = Net Mass Accumulation of Component *i* with Time (1)

For component *i* being a compressible fluid typically a gas, the derived expression is limited to only free gas phases. Accounting for solution gas term in each of the coordinates, since retrograde condensation phenomenon starts at pressures below P_{dew}, the deduced equation is presented as;

$$\frac{\partial}{\partial x}\left[\left(\beta\frac{k_{gx}}{B_g\,\mu_g}Ax\left(\frac{dP}{dx}-\gamma_g\frac{\partial \mathbb{N}}{\partial x}\right)\right)+\left(-\beta\frac{k_{ox}}{B_o\,\mu_o}Ax\,R_{so}\left(\frac{dP}{dx}-\gamma_o\frac{\partial \mathbb{N}}{\partial x}\right)\right)\right]\Delta x +$$
$$\frac{\partial}{\partial y}\left[\left(\beta\frac{k_{gy}}{B_g\,\mu_g}Ax\left(\frac{dP}{dy}-\gamma_g\frac{\partial \mathbb{N}}{\partial y}\right)\right)+\left(\beta\frac{k_{oy}}{B_o\,\mu_o}Ax\,R_{so}\left(\frac{dP}{dy}-\gamma_o\frac{\partial \mathbb{N}}{\partial x}\right)\right)\right]\Delta y +$$
$$\frac{\partial}{\partial z}\left[\left(\beta\frac{k_{gz}}{B_g\,\mu_g}Ax\left(\frac{dP}{dz}-\gamma_g\frac{\partial \mathbb{N}}{\partial x}\right)\right)+\left(\beta\frac{k_{oz}}{B_o\,\mu_o}Ax\,R_{so}\left(\frac{dP}{dz}-\gamma_o\frac{\partial \mathbb{N}}{\partial z}\right)\right)\right]\Delta z + (q_{sc}s') = \frac{V_b\,\emptyset\ \ T_{sc}}{\alpha T\,Z_i\,P_{sc}}\frac{\partial P}{\partial t} \quad (2)$$

Where;

$$q_{sc}s' = s'q_{gsc} + s'q_{csc}\,R_{so}$$

Since two phases (oil and gas) are accounted for in Equation (2), it is convenient to express the above transport equation in terms or relative permeabilities.
For the free gas component, the effective gas permeability in all three coordinates is given as;

$$k_{gx} = k_x k_{rgx};\quad k_{gy} = k_y k_{rgy}\ \text{ and }\ k_{gz} = k_z k_{rgz}$$

For solution gas in oil component

$k_{ox} = k_x k_{rox}; \quad k_{oy} = k_y k_{roy}$ and $\quad k_{oz} = k_z k_{roz}$

Hence, Equation now becomes

$$\frac{\partial}{\partial x}\left[\left(\beta\frac{k_x k_{rgx}}{B_g\,\mu_g}Ax\left(\frac{dP}{dx} - \gamma_g\frac{\partial \mathbb{N}}{\partial x}\right)\right) + \left(\beta\frac{k_x k_{rox}}{B_o\,\mu_o}Ax\,R_{so}\left(\frac{dP}{dx} - \gamma_o\frac{\partial \mathbb{N}}{\partial x}\right)\right)\right]\Delta x +$$
$$\frac{\partial}{\partial y}\left[\left(\beta\frac{k_y k_{rgy}}{B_g\,\mu_g}Ax\left(\frac{dP}{dy} - \gamma_g\frac{\partial \mathbb{N}}{\partial y}\right)\right) + \left(\beta\frac{k_y k_{roy}}{B_o\,\mu_o}Ax\,R_{so}\left(\frac{dP}{dy} - \gamma_o\frac{\partial \mathbb{N}}{\partial x}\right)\right)\right]\Delta y +$$
$$\frac{\partial}{\partial z}\left[\left(\beta\frac{k_z\,k_{rgz}}{B_g\,\mu_g}Ax\left(\frac{dP}{dz} - \gamma_g\frac{\partial \mathbb{N}}{\partial x}\right)\right) + \left(\beta\frac{k_z k_{roz}}{B_o\,\mu_o}Ax\,R_{so}\left(\frac{dP}{dz} - \gamma_o\frac{\partial \mathbb{N}}{\partial z}\right)\right)\right]\Delta z + (q_{sc}s') =$$
$$\frac{V_b\,\emptyset\quad T_{sc}}{\alpha\,TZ_i\;\;P_{sc}}\frac{\partial P}{\partial t} \tag{3}$$

The simplified gas predictor model in Equation (3) is given as ;

$$\frac{\partial}{\partial x}[(A) + (B)]\Delta x + \frac{\partial}{\partial y}[(C) + (D)]\Delta y + \frac{\partial}{\partial z}[(E) + (F)]\Delta z + \dot{Q}_{skin} = H \tag{4}$$

Where;

$$\mathbf{A} = \beta\frac{k_x k_{rgx}}{B_g\,\mu_g}Ax\left(\frac{dP}{dx} - \gamma_g\frac{\partial \mathbb{N}}{\partial x}\right); \quad \mathbf{B} = \beta\frac{k_x k_{rox}}{B_o\,\mu_o}Ax\,R_{so}\left(\frac{dP}{dx} - \gamma_o\frac{\partial \mathbb{N}}{\partial x}\right); \quad \mathbf{C} = \beta\frac{k_y k_{rgy}}{B_g\,\mu_g}Ax\left(\frac{dP}{dy} - \gamma_g\frac{\partial \mathbb{N}}{\partial y}\right)$$
$$\mathbf{D} = \beta\frac{k_y k_{roy}}{B_o\,\mu_o}Ax\,R_{so}\left(\frac{dP}{dy} - \gamma_o\frac{\partial \mathbb{N}}{\partial x}\right); \quad \mathbf{E} = \left(\beta\frac{k_z k_{rgz}}{B_g\,\mu_g}Ax\left(\frac{dP}{dz} - \gamma_g\frac{\partial \mathbb{N}}{\partial x}\right)\right); \quad \mathbf{F} = \beta\frac{k_z k_{roz}}{B_o\,\mu_o}Ax\,R_{so}\left(\frac{dP}{dz} - \gamma_o\frac{\partial \mathbb{N}}{\partial z}\right);$$
$$\dot{\mathbf{Q}}_{\mathbf{skin}} = (q_{sc}s')\;; \quad \mathbf{H} = \frac{V_b\,\emptyset\quad T_{sc}}{\alpha\,T\,Z_i\;\;P_{sc}}\frac{\partial P}{\partial t}\;; \quad \mathbf{s'} = s + D'q_{gsc}\;; \quad \mathbf{D'} = \frac{6\times10^{-5}\,\gamma_i\,k_s^{-0.1}\,h}{\mu_i\;\;r_w\,h_p^2}$$

2.4: Relative Permeability Evaluation

Above the dew point (saturation pressure of condensates) where a single-phase system exists, we assume a 2-phase flow of gas and water (though predominantly gas, provided the connate water saturation is low and the assumption that the reservoir rock is water wet strongly holds). The flow of each phase is dependent on the relative permeabilities of each another, which is a function of the phase saturations and the wetting properties of the individual phases. Below the saturation pressure, the retrograde condensation phenomenon begins to occur and an – gas system begins to form. Willie and Gardner's correlation which proves more specific to the study area was used for this analysis. Still putting into consideration the unconsolidated well-sorted nature of the reservoir sand (for which the Niger Delta is characterized), the respective relative permeabilities of gas and liquid (condensate) is given as;

$k_{rg} = \left(1 - S_g^*\right)^3$ and $k_{rc} = (S_c^*)^3$

Also representing the condensate relative permeability, k_{rc} when k_{rg} is known we adopt;

$k_{rc} = (S_c^*) - k_{rg}\left[\frac{S_c^*}{1-S_c^*}\right]$

Where $s_o^* = \frac{s_o}{1-s_{wi}}$; $s_g^* = \frac{s_g}{1-s_{wi}}$

2.5 PVT Modeling and Solution Techniques

PVT parameters were generated from CVD and CCE analysis using the *PVTp* Petroleum Expert simulator. This was done by obtaining rock and fluid data from a Niger Delta Condensate field and running series of raw data inputs to extract these PVT parameters. Characterization of the reservoir was executed by adopting appropriate viscosity correlations, gas deviation factor correlations, the Peng-Robinson's Equation of state, Glasso Solution gas correlation, implementing field separator conditions and separator fluid properties including;

separator oil gravities, gas gravities, pressure, temperature, fluid densities and liquid – gas ratios were all raw inputs for the PVT modeling at reservoir conditions. EOS tuning was used to obtain a series of relationships generated by variation in some PVT properties, this was done to simulate and estimate accurate reservoir conditions since accurate representative sampling from a gas condensate reservoirs proved difficult.

All solutions adopted for this work were aimed at utilizing parameter refinement techniques to attaining maximum convergence in obtained results. These techniques include; Finite difference approximation schemes which when resolved will generate a series of linear algebraic equations that will be solved using Gauss–Siedel iterative method. High precision relaxation techniques such as the Successive Over-Relaxation method (SOR) was adopted to accelerate and speed up the convergence of deduced pressure values for the Gauss-Seidel solutions at every position for various time steps. The convergence of pressure deductions in both the spatial and time domains was achieved by Gauss-Seidel techniques and accelerated by adopting the Point SOR. This was achieved by refining the values of the estimated unknowns to reduce the number of iterations required for convergence.

$$x_i^{k+1} = (1-\omega_{opt})x_i^{(k)} + \frac{\omega_{opt}}{a_{ij}}\left[b_i - \sum_{j=1}^{i-1} a_{ij}x_j^{(k+1)} - \sum_{j=l+1}^{n} a_{ij}x_j^{(k)}\right] \qquad (5)$$

Where i = 1, 2, 3, 4…….n

Optimum relaxation parameter $\omega_{opt} = \frac{1}{(1+\sqrt{1-\sigma})}$ and is problem specific. The value of ω_{opt} is usually obtained when the matrix for the problem set is generated during model resolution.

2.6 Adopting the Predictor Model to Candidate Reservoir Conditions (Study Area)

The gas condensate reservoir with homogenous formation sand of porosity 22.1% covers a total area of 22.76 square – KM (5,624.43 acres) with boundary – specific pressures adequately defined. The hydrocarbon-water contact (HWC) was recorded at a depth of 12,100 ft from the tree–valve and the initial pressure and production rate for the gas reservoir was 4991.7 psi and 55 MMscf respectively. The sandstone reservoir is well sorted, thin, uniform, horizontal, dipping at an angle of 180^o, and has a surface GCR of 21470.7 scf/STB.

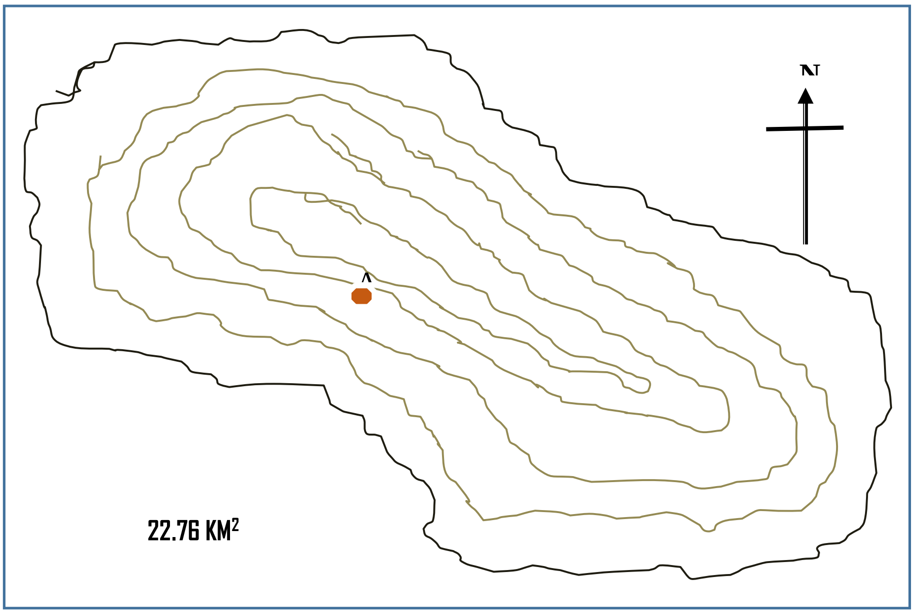

Figure 2: Surface Map of Gas Condensate Reservoir

Consider the surface map of the reservoir in Figure 2 above with a producer located at point-A. A Block Centered Gird System (BCGS) is adopted and superimposed on the above reservoir for proper discretization. An average of 20 hypothetical grids is generated as shown in Figure 3, each with an average area of 12.25 × 10^6 ft^2 with pressure and saturation evaluation conducted for all 20 grids. The sum of the total number of grids cumulatively adds up the total surface area of the reservoir.

Model Assumptions

- The reservoir sand is an unconsolidated, well-sorted system and is completely uniform, homogenous and isotropic.
- The reservoir is free from a significant amount of impurities (H_2S, CO_2 & N_2), and as such, mole percent of these non-hydrocarbon components in reservoir fluid stream considered negligible.
- Skin analysis of the reservoir is evaluated only in the producing well grid.
- The gas injection rate is maintained throughout the injection period.
- Injection gas composition is either similar to the reservoir fluid composition, with a higher percentage of lighter fractions or sequestered CO_2.
- The reservoir is perfectly horizontal with no dip ($\vartheta = 180$), implying that there is no elevation component and analysis will be limited to 2 dimensions alone.
- Bottom aquifer pressure support is inadequate for pressure maintenance.
- No reservoir structural features (faults, folds etc.).
- Flow is unsteady, turbulent, and predominantly in the x and y coordinates.

Figure 3 below shows node designation and the implementation of superimposed hypothetical grid blocks for pressure and saturation evaluation.

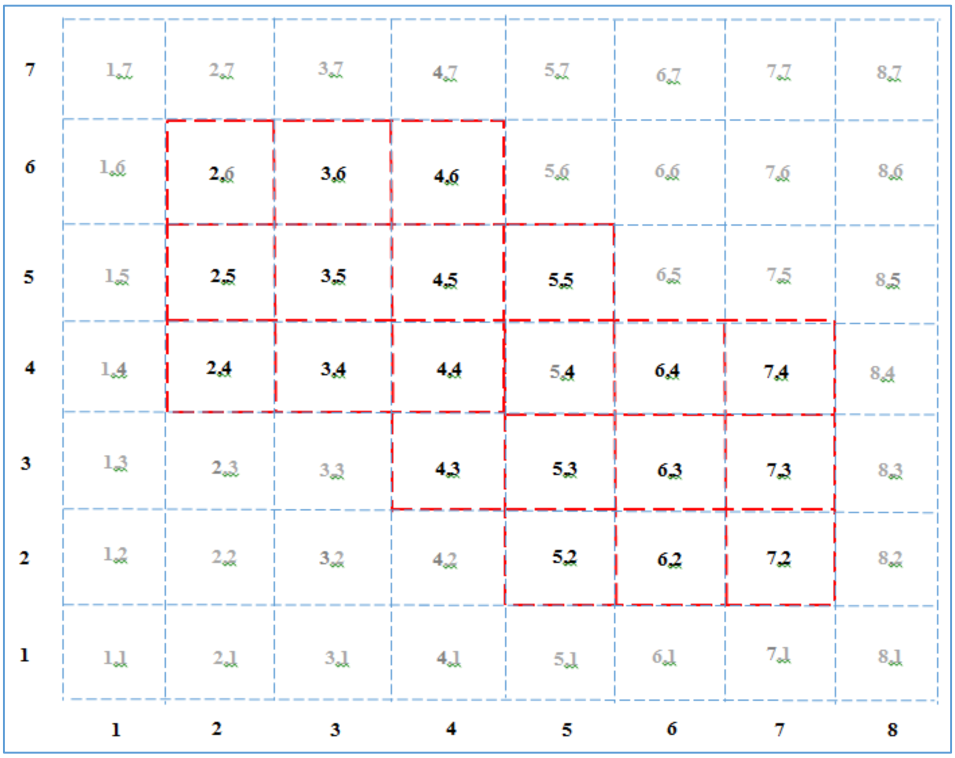

Figure 3: Node Designation Showing Superimposed a Block Centered Hypothetical Grid on the Gas Condensate Reservoir

Working on the assumption that there is no dip (i.e., no z-vector) and that flow is predominant in the x – y directions and formation conductivity (kh) to flow is highest in both directions (reservoir has an evenly distributed vertical and horizontal permeability), the 3-Dimensional model is reduced to a dual-coordinate system given as;

$$P_{x-1,y}^{n+1} + P_{x+1,y}^{n+1} + P_{x,y-1}^{n+1} + P_{x,y+1}^{n+1} - [4 + L_1]P_{x,y}^{n+1} = -L_1\left(P_{x,y}^{n}\right) - L_2\left(q_{gsc}s'\right) \quad (6)$$

The implementation of skin factor *s'* is solely on the assumption that only producing well blocks are affected and hence, damage implication for injection well blocks will not apply.

2.7 Reservoir Simulation and Sensitivity Analysis

Having successfully transformed the parabolic Partial differential equations into its implicit finite Difference equivalent and substituting the obtained near – accurate reservoir fluid and rock properties such as (viscosities of each phase, phase formation volume factors at initial conditions, reservoir gas solubility, reservoir gravities of the respective phases, compressibility factors and reservoir phase densities) via PVT modeling, the MS-Excel VBA program code was written for Gauss–Seidel iterative solution to deduce pressure values at each grid for defined time steps. The successive-overrelaxation implementation was also encoded to the characteristic system of linear equation using the Iterative – Solving (IS) function for a more rapidly accelerated convergence to the actual pressure values for the reservoir grids.

Reservoir heterogeneities and non-isotropic conditions can initiate drastic pressure drops within the porous media particularly for gas condensate reservoirs. Sensitivity analysis was performed on the pressure/saturation predictor model to ascertain the effects of variation in the magnitude of skin (formation damage) or permeability impairment predominantly around the region with the lowest pressure (the wellbore). These variations will be in the magnitude of s = 2.5, s = 5.0, s = 7.5 , s = 10.0 and s = 12.5

III. RESULTS AND DISCUSSION

3.1 Relative Permeability Evaluation

The Wyllie and Gardner relative permeability correlation for an unconsolidated, well-sorted sandstone formation was also used to perform the Rel-Perm analysis. It was observed that there is a considerable distinction in relative permeability quantification with the Corey correlation at the same liquid and gas-phase saturations. Putting into account the formation type, initial gas, and oil phase saturations for the Niger Delta case, a lower estimated gas relative permeability, k_{rg} is obtained when compared to the Corey evaluation. This variation in k_{rg} estimation could be as a result the unified (all formation type) application of the Corey relative permeability correlation as it does not take into consideration, type of formation for which the saturating fluids are been evaluated.

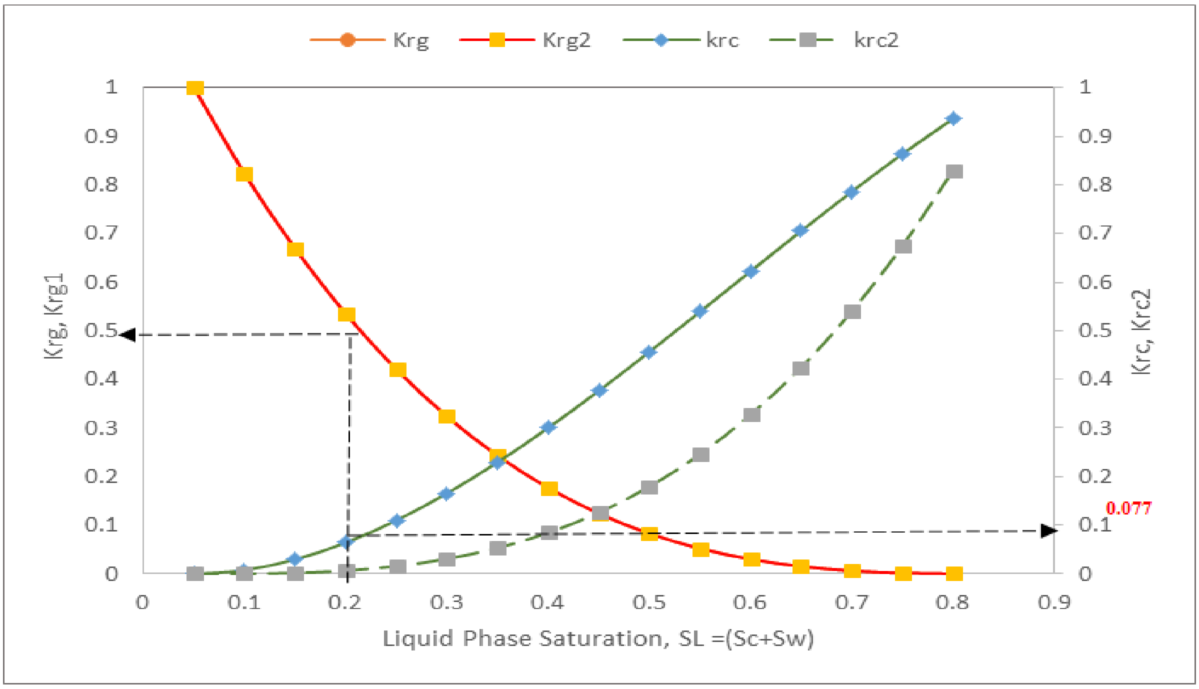

Figure 4: Wyllie and Gardner Deduced Relative Permeability for Gas for the Unconsolidated, Well-Sorted Niger Delta Sandston Formation

As shown in Figure 4, the Wyllie and Gardner correlation presents a variation in k_{rg} and k_{rl} with liquid phase saturation and tends to predict a 0.5 relative permeability of gas at 77.89% initial gas saturation. The corresponding liquid relative permeability at the initial liquid saturation of 21.01% is 0.077. This observation implies that for this sandstone formation, at higher gas saturations, the dynamics of the reservoir system will principally be dominated by the gas phase. This also implies that the effective permeability of gas in the system will dominate almost half the absolute permeability of the sandstone reservoir. The low effective permeability of the liquid phase as deduced from the above system will to a large extent make up a bulk fraction of the stationary phase of the fluid system having just about 0.077 fractions of the absolute permeability of the sandstone formation. Condensates most times have such behaviors as they tend to exist in isolated droplets sparsely dispersed across the reservoir in areas with reservoir pressure equal to or below the saturation pressure (due point pressure). The second liquid relative permeability curve, k_{rl2} shows the relative permeability behavior for a poorly sorted, unconsolidated sandstone formation. At the same initial liquid saturation of about 20.01% the corresponding liquid relative permeability is approximately 0.025 as against 0.077 for the well-sorted, unconsolidated sandstone formation. This implies that the evaluation of liquid phase effective permeability for a poorly sorted – unconsolidated sandstone formation will yield a lower magnitude of liquid permeability in the system than a well-sorted, unconsolidated formation at the same phase saturation.

3.2 PVT Modeling and Depletion Studies for the Gas Condensate Reservoir

For the 13–component system, the IPM suite *PVTp* software was used to model for PVT parameters, generate a series of reservoir behavior for depletion studies, and obtain accurate reservoir characterization. Before initiating PVT modeling, the software option was programmed to engage the Peng – Robinson EOS, Lohrenz – Bray – Clark correlation for viscosities and Standing – Katz oil density correlation. Primarily, requirements for data inputs were reservoir pressure of 4991.7 psia, initial reservoir temperature of 221°F, and a reservoir reference depth from the surface of 12,100 ft. Reservoir characterization revealed that the system was a dew point system (Gas condensate reservoir system). Further characterization established a cricondenterm, T_{ct} and cricondenbar, P_{cb} of 422.1 ^oF and 3816.00 psia respectively. The critical properties of the gas condensate reservoir system via the phase envelope with critical pressure and critical temperature of 3775.11 psia and 219.1 ^oF respectively is shown in Figure 5 below.

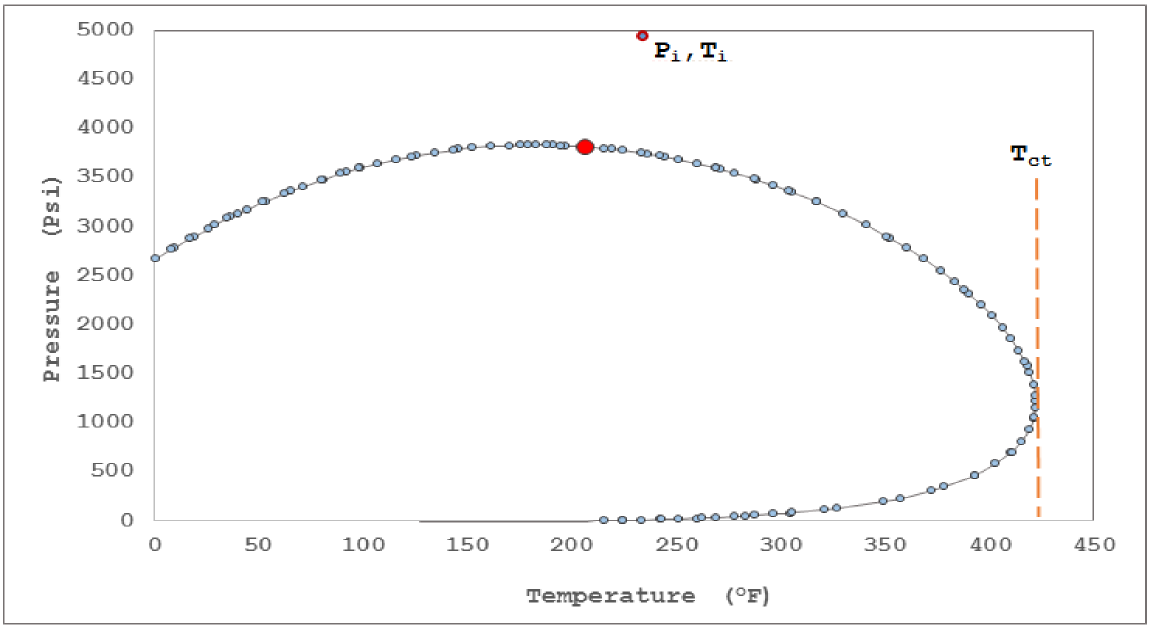

Figure 5: Phase Envelope for the Near – Critical Gas Condensate Reservoir

The above-deduced phase envelope shows a typical dew point reservoir for which the initial reservoir temperature of 221^{o}F lies between the critical temperature, T_c of 219.1^{o}F, and cricondenterm T_{ct} of 422.1^{o}F. The P – T relationship or frequently called the phase envelope was generated from the deductions of pressure-temperature functions embedded in the simulator after characterization. Black oil properties of the reservoir record a GOR of 5541.16 scf/STB (for which lies GOR for gas condensates lies between 5000 – 70,000 scf/STB), CGR of 180.47 STB/MMscf, oil gravity of 84.84^{o}API and so on.

3.2.1 CCE Analysis and CVD Analysis

Depletion performance and compositional variation studies for the reservoir stream was also conducted using the CVD evaluation and the CCE analysis to accurately simulate pressure-volume relationships on reservoir isothermal depletion.

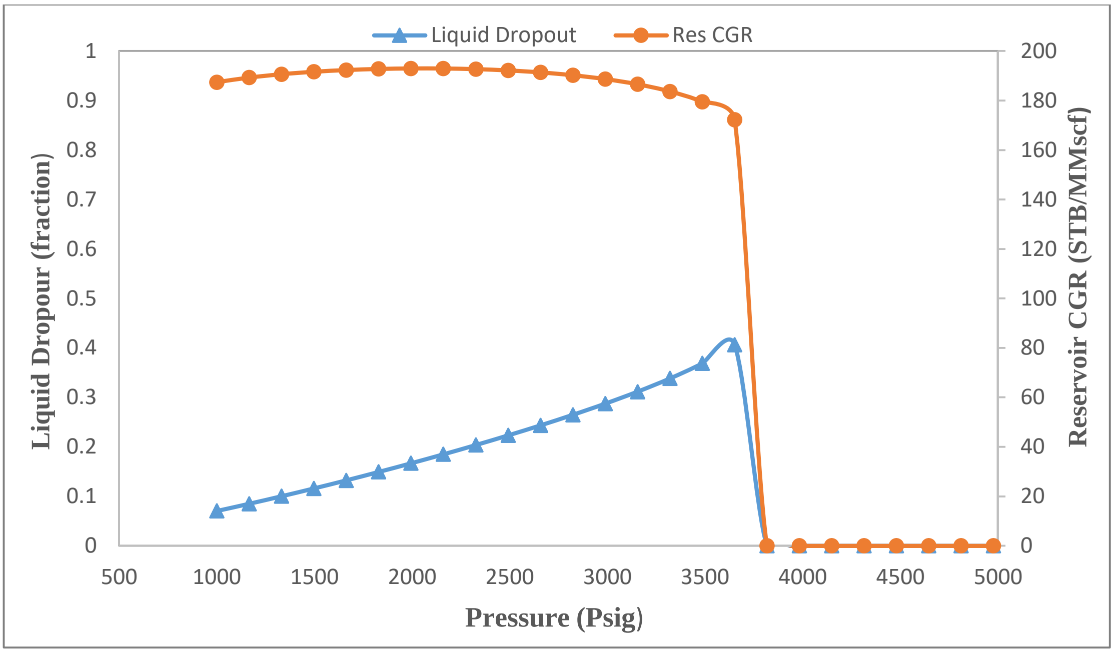

Figure 6: Condensate Dropout Fraction and Condensate – Gas Ratio as a Function of Pressure from CCE Evaluation.

Figure 6 above presents the variation in reservoir condensate – gas ratio (CGR) and liquid fraction drop out of the heavy ends with pressure depletion. Here, it is observed that for pressures above the saturation pressure (dew point pressure) 3825.86 psia, there exists a single-phase gas system and a zero liquid dropout fraction. This also translates to the CGR as it records a zero magnitude because there are no condensates formed at these pressure ranges. At pressures below the dew point pressures, as observed in the figure, there is a sharp increase in the fraction of condensate dropout of 0.41 with a corresponding increase in the CGR of 172.27 STB/MMscf both at a pressure of 3651.33 psia where the highest dropout is observed in the reservoir system. The CVD deductions revealed that as an isothermal depletion occurs in the reservoir, gas recovery fractions will reduce with time and the condensate recovery fraction will increase accordingly. However, for pressures above the dew point pressure, there will be no oil recovery as a result of the gas phase predominance in the total dynamics of the reservoir system. Continuous reduction in pressure yields the gradual drop out of the liquid phases as observed from the CCR analysis.

Figure 7 below validates that the highest condensate recovery will be recorded at reservoir locations with lower pressure values. This however poses a problem in the recovery of the total hydrocarbon from such reservoirs as increased condensate volumes may restrict the gas flow and production upon reservoir depletion.

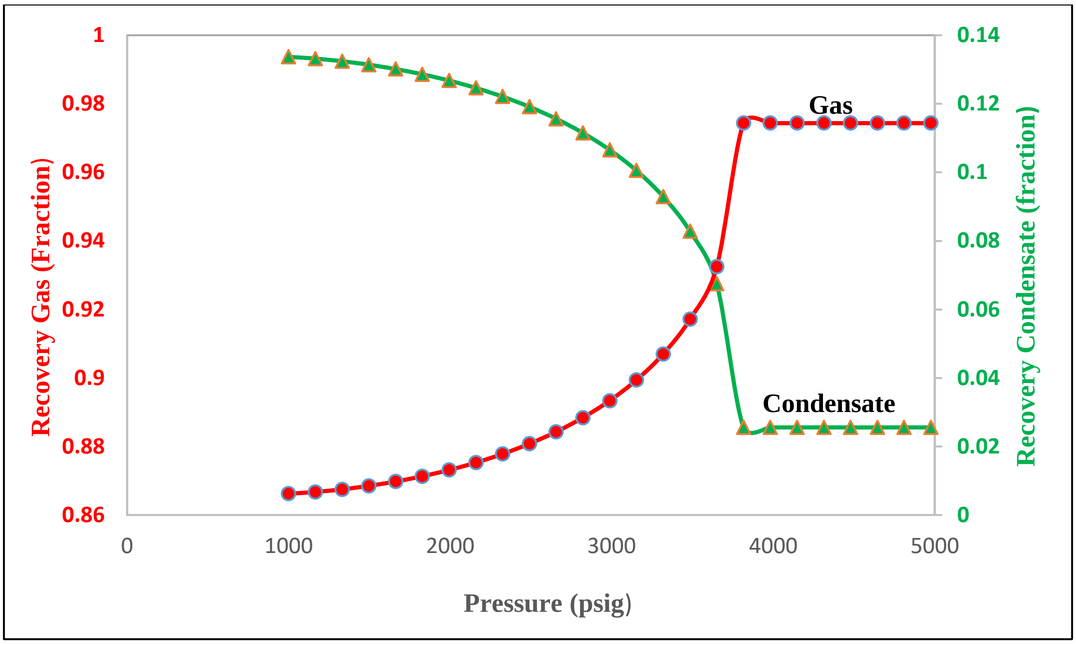

Figure 7: Condensate Recovery and Gas Recovery Fractions as a Function of Pressure from CVD Evaluation

3.3 Parameter Refinement with SOR

Having accurately linearized the partial differentials into sets of linear algebraic equations with 20 pressures unknown, pressure deductions were made in the spatial domain at the first time level by rewriting the linearized equations in its SOR equivalent. The designated optimum relaxation parameters of 1.25, 1.30, and 1.35 all displayed high-level spatial pressure convergence with the only difference all three being the number of iteration runs and time of convergence. Table 4.1 presents a summary of the effect of the variation of the optimum relaxation factor on the number of iterations.

Table 1: Effect of Variation in ω_{opt} on Convergence Duration

	Optimum Relaxation Factor, ω_{opt}			
	1	**1.25**	**1.30**	**1.35**
Number of Iterations	21	15	12	17
Percentage Error	1.99×10^{-7}	1.99×10^{-7}	1.99×10^{-7}	1.99×10^{-7}

3.4 Validity of the Predictor Model

Since the skin–incorporated, the multi-dimensional model is novel, validation, and assertion of model credibility poses a problem in its general acceptability and applicability. However since there is a conventionally used 3 - D model for pressure distribution, though it tends to neglect the integration of the influence of formation damage, served as a powerful tool for the validation of the proposed pressure/saturation predictor equation. However, the predictor equation is reduced to assume a no – skin function to match the conventional 3 – D model with both computed with $\omega_{opt} = 1.30$.

Before the proposed model could serve as a tool for pressure profile forecast, validation via matching with a reference was conducted and the trend/profile of the match is analyzed. The figure below shows the trend for both the conventionally used model and the predictor equation.

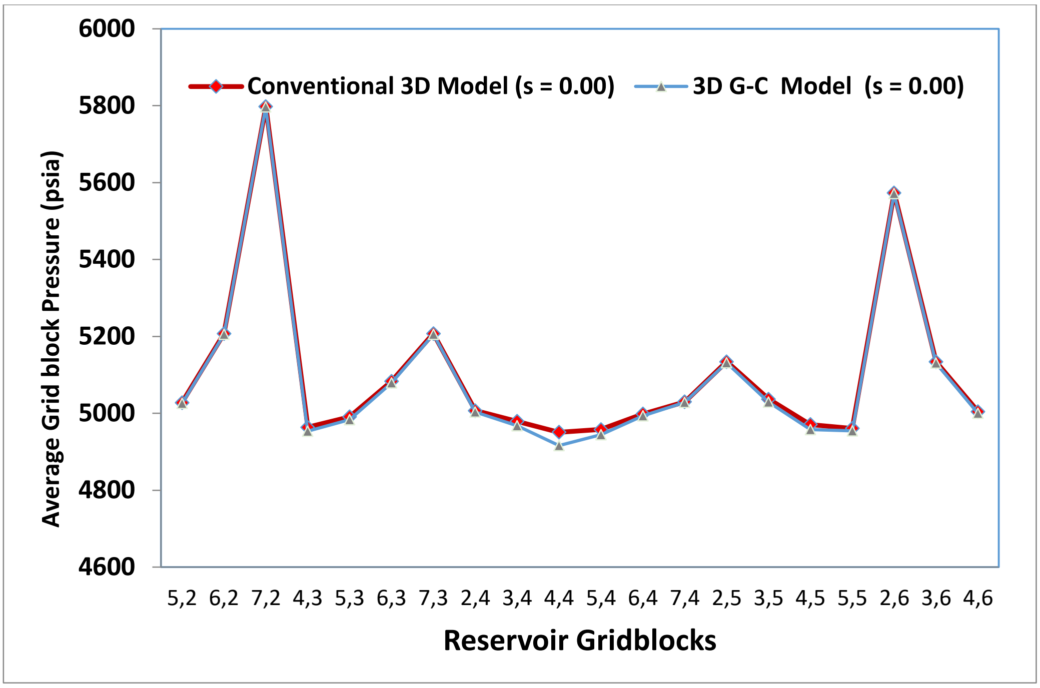

Figure 8: Predictor Model Validation with Conventional Pressure Distribution Model

Here, it is observed that there is a close match in pressure distribution in the grid blocks across the reservoir, having same production rates, injection rates, reservoir rock and fluid properties with the only exclusion of the skin component and non – Darcy turbulence factor in the predictor equation. Having been validated via pressure profile and observing trend across the 20 grid blocks, the predictor model can hence be a useful tool in production forecasting and sensitivity analysis can be conducted to ascertain the effects of various skin magnitudes of pressure and saturation profiles for the Niger Delta Gas condensate systems.

From Figure 9 below, it is observed that the higher the magnitude of skin, the lower the average pressure in the production grid block. Assuming the effect of skin is neglected, (for which the conventional pressure distribution model is adopted), an average pressure of 4950.77 psia is recorded in grid 4,4. For the predictor model, an additional pressure drop of about drifting 34.25 psia less than the former, possibly as a result of fines migration and accumulation within the wellbore vicinity (producing block) due to the unconsolidated nature of the Niger Delta sandstone formation yielded an average of 4916.52 psia in the same block. Skin magnitudes of 2.00, 2.50 and 3.00 recorded an average pressure in grid block 4,4 of 4912.72 psia, 4903.21 psia, and 4884.18 psia respectively.

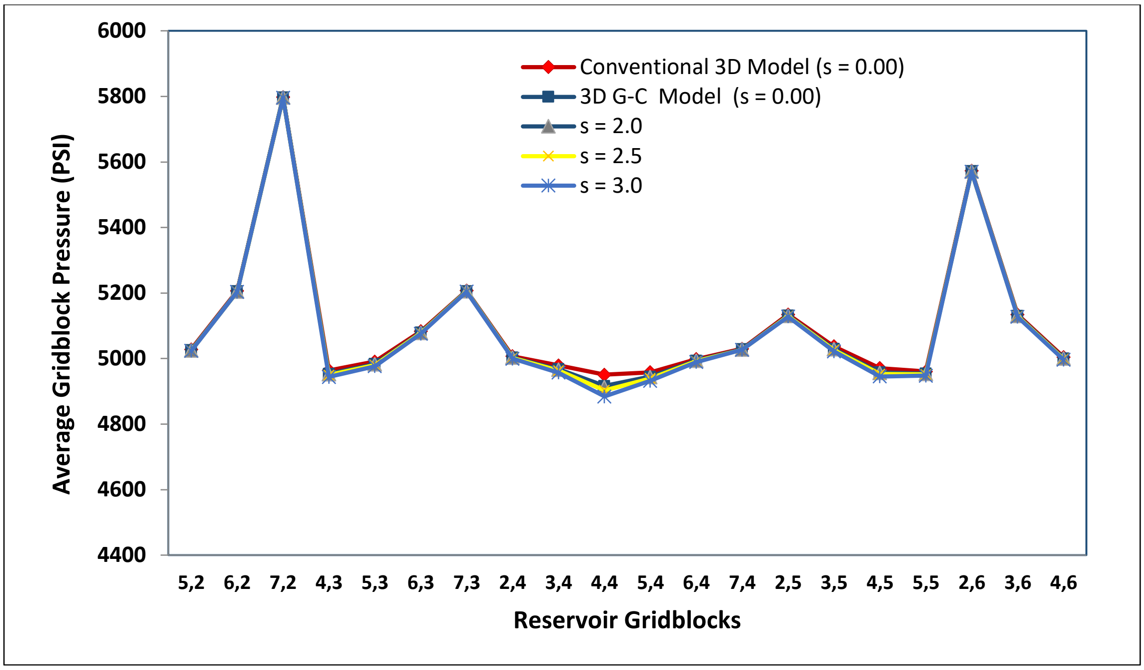

Figure 9: Increase in Pressure Drop at Producing Well block with Increasing Magnitudes of Skin at Δt = 15.21 days.

3.5 Performance Prediction of Reservoir

3.5.1 Spatial Evaluation

Following validation, the gas condensate reservoir performance can then undertake a series of performance prediction evaluations to inform good ecumenical investment decisions, production forecast, condensate reservoir surveillance/monitoring and prompt the maximization of optimum condensate recovery techniques for a Niger Delta case scenario.

3.5.1.1 Reservoir Performance with no Injector

The pressure profile for the gas condensate reservoir is below shows the pressure distribution across the grids for a system without pressure maintenance.

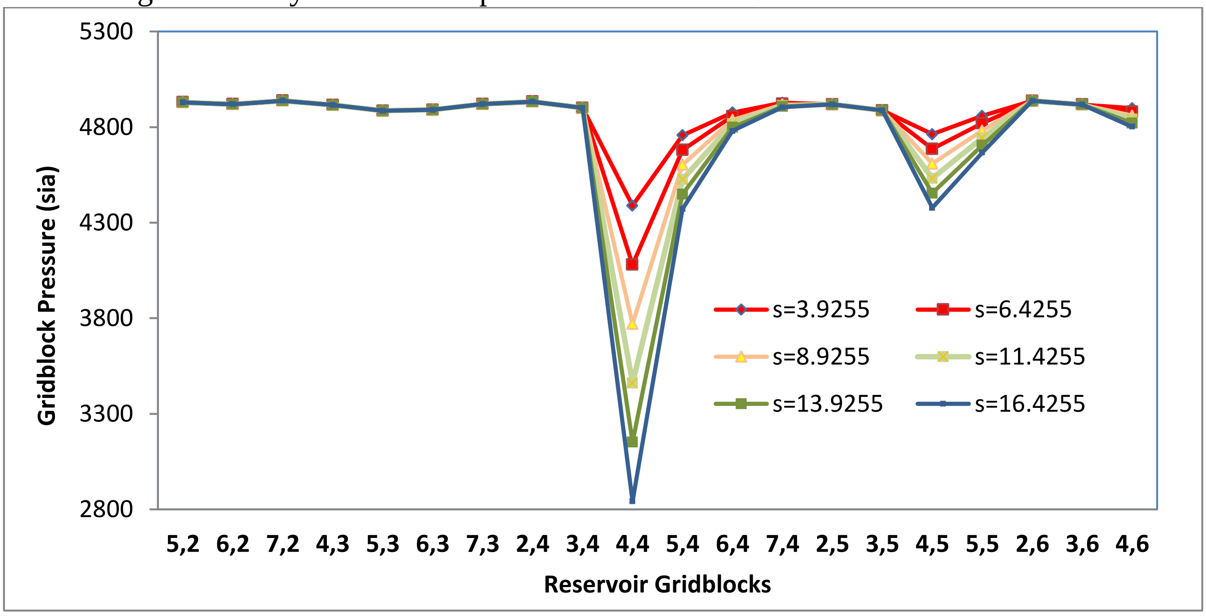

Figure 10: Effect of Variation in Formation Damage Magnitudes on Pressure Profile after 15.21 days of Production (No Pressure Maintenance)

Here, it is observed that for a production period of 15.21 days, the production well block can maintain a single-phase gas stream for skin values of 3.9255 and 6.9255, with pressures of 4389.38 psia and 4079.27 psia respectively, both far above the saturation pressure of 3817.04 psia. At skin values of 13.9255 and 16.4255, severe condensate banks had been formed since both pressures are far below saturation pressure. Skin magnitudes of 11.4255 and 8.9255 with respective well block pressures of 3151.17 psia and 3460.72 psia can be classified as Region 2 condensate systems according to Roussennac, 2001. This region lies between the severe condensate bank and the single gas phase system. Surrounding grid blocks to the producing block such as gridlocks 4,5, 5,5, 3,4, 5,4 and 4,6 also is affected by the influence of the well block as they showed significant drops in pressure but still maintained at a single gaseous phase all having pressures above the dew point pressure of 3817.04 psia. Conclusively, it can be inferred that formation damage intensity above the 6.4255 magnitude can incur condensate banking problems for a Niger Delta sandstone formation, if pressure support schemes are not made available.

3.5.1.2 Reservoir Performance for a Single-Injector System

For a system with one injector located in grid block **7,2**, with an injection rate of 54.28 MMMscf/day, it is observed in Figure 11 that there is an increase in the average pressure across the reservoir as compared to the depletion case above with no pressure support. However, in as much as the injection process supplies the required rate for pressure maintenance via material balance principle, the producing block still records the same trend as the above case scenario with the only exception being higher values of recordable pressure at **4,4**. This translates that despite the pressure support available, a single injector cannot adequately maintain a constant and evenly distributed pressure support to the entire system.

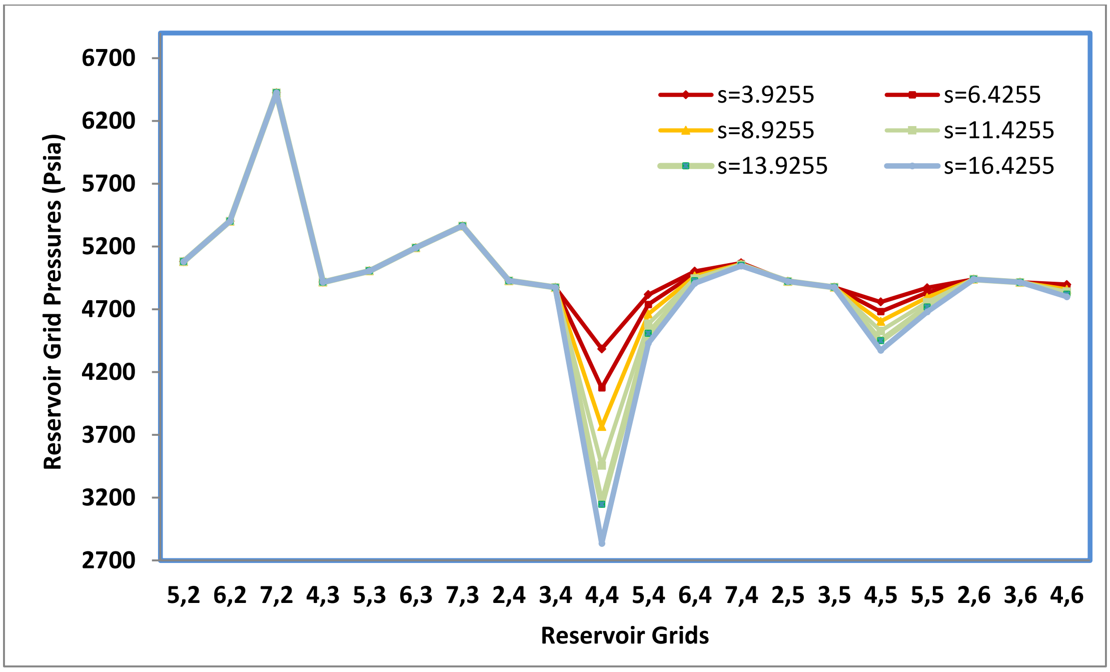

Figure 11: Effect of Variation in Formation Damage Magnitudes on Pressure Profile after 15.21 days of Production (Pressure Maintenance with Single Injector).

For this single injector case, a skin magnitude of 8.9255 can be accommodated since its pressure of 3765.38 psi in the producing well block hovers around the 3817.04 psi saturation pressure. Here, production optimization of the reservoir can be achieved as an intermittent gas lift technique can be considered due to its proximity to a single-phase gaseous system in the producing block. A possible reason for the non-effective dispersion of pressure across the reservoir grids could be that the injection well block pressure of 6423.00 psi far exceeds the fracture pressure threshold of the reservoir rock and as such, a sharp pressure drop occurs in surrounding areas as a result of artificial fractures been created. Therese sudden pressure surge is tantamount of incurring condensate banking if not properly monitored.

3.5.1.3 Reservoir Performance with a Dual-Injector System

For the gas condensate reservoir, it is observed to be the most ideal reservoir exploitation option as it tends to supply much better than the single injector case, a substantial pressure distribution across the reservoir gridlocks. As shown in Figure 12, a skin Magnitude of up to 8.9255 can comfortably maintain a single-phase gaseous phase without a retrograde condensation phenomenon as it records an average pressure of 3825.55 psia for the producing well block which is comparatively higher than the dew point pressure of 3817.04 psia.

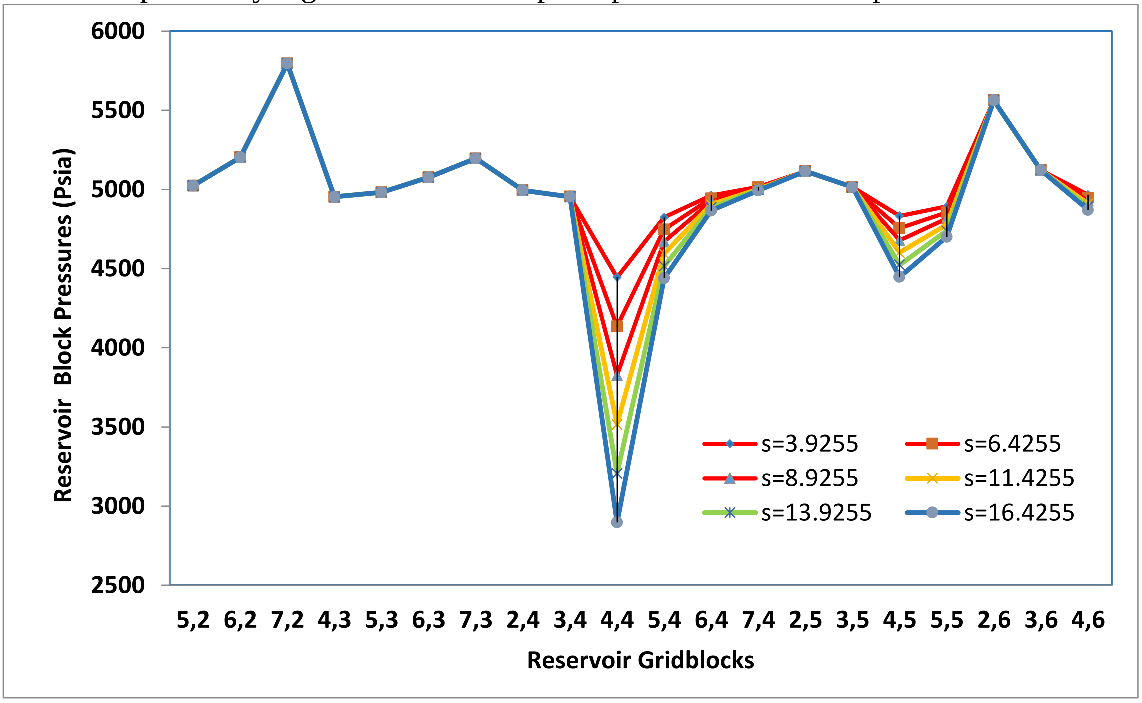

Figure 12: Effect of Variation in Formation Damage Magnitudes on Pressure Profile after 15.21 Days of Production (Two-injector Pressure Maintenance).

Formation damage (skin) magnitudes of 11.4255 as shown in Figure 12 above reveals that a 2 phase mixture of gas and liquid will exists as the average pressure in the block records 3515.99 psia. The 3206.44 psia and 2896.88 psia for their corresponding damage magnitude of 13.9255 and 16.4255 will be classified as severe condensate bank phenomenon because at these pressures ranges, only single-phase liquid system may exist in the producing block. This is capable of killing the gas well as gas lift artificial lift methods may not adequately maximize production at these formation damage (skin) ranges.

3.5.2 Reservoir Stepwise Evaluation (Production Forecast)

3.5.2.1 Reservoir Performance for Skin Magnitude of 3.9255

3.5.2.1.1 No Pressure Maintenance

Any gas condensate reservoir under production without a pressure maintenance scheme is prone to early banking effects in its production grid block. In this case, production is maintained in grid block **4,4** above saturation pressure of 3817.04 until 61 days were production grid block pressure was 3825.86 psia after which it dropped to 3801.97 psia after the next 15.21 days of observation. It can however be inferred that if pressure is not maintained for this reservoir with a damage magnitude of 3.9255, a single-phase production of gas can only be achieved for at most 76 days if production is maintained at a constant rate.

3.5.2.1.2 Single Injector Pressure Maintenance

The one-year pressure profile for the production grid shown in Figure 13 for a skin magnitude of 3.9255 reveals that grid block **4,4,** all things being equal, can conveniently maintain a withdrawal rate of 55MMscf/day of single-phase gas without the possibility of condensate baking.

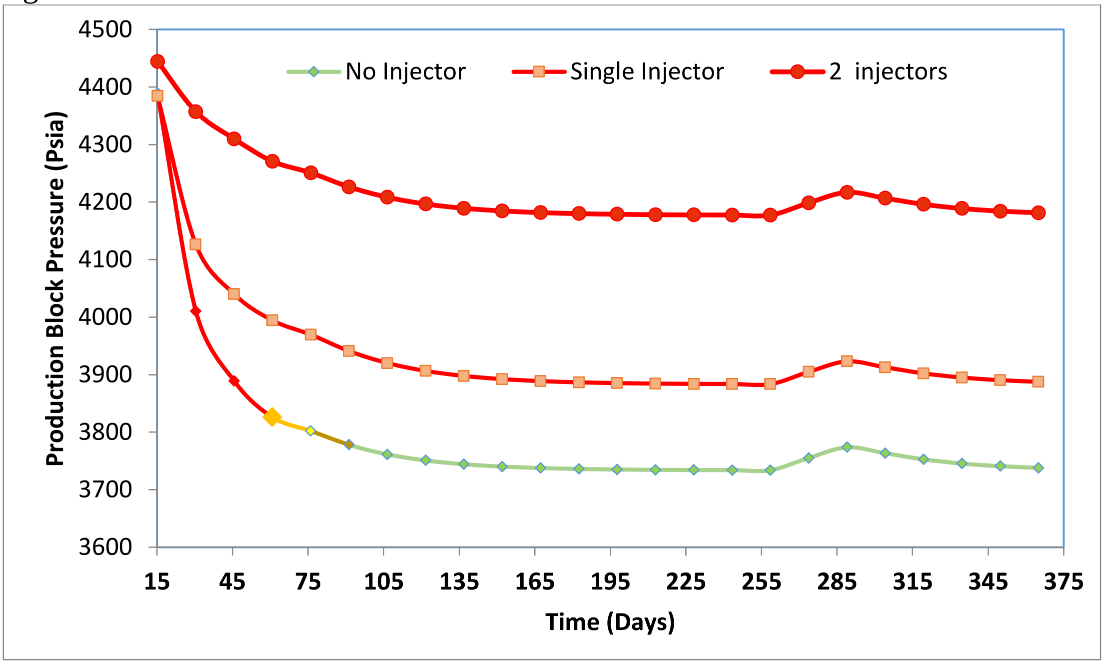

Figure 13: One-Year Pressure Forecast for the Production Well Block with a Skin Magnitude of 3.9255 for Different Pressure Maintenance Scenarios.

This is because the one year forecast all have pressure predictions far above the dew point pressure, with its lowest pressure of 3887.30 psia recorded after 365 days of production. The reason for this being that; provided the pressure maintenance evaluation via MBE is accurately calculated, pressure response throughout the reservoir will be sufficiently accounted for.

3.5.2.1.3 Pressure Maintenance with Two (2) Injectors

A single injector can conveniently maintain production block pressure for a 365 day production period depicted in figure 12. This to a large extent may be inadvisable because an injection rate of 54.28 MMMscf/day may be speculated to cause a "frac" effect on the sandstone formation since the injection is continuous. This as earlier stated can incur sudden pressure drops at the injector blocks which will in turn bring about the retrograde condensate phenomenon. To mitigate this prospective problem, a 2 – injector system is suggested for an even distribution of pressure (more like a safety consideration). Surface pumping equipment will have less operational resistances to deliver the required injection rates efficiently. Having accurately determined injection rates and strategically locating injectors at suitable positions, a higher production block pressure can be achieved far higher than that of a single well injection process. A minimum predicted pressure of 4818.52 psia after 365 days in grid block **4,4** at a skin magnitude of 3.9255 far supersedes a single injector system which predicts 3887.30 psia after 365 days for same skin magnitude.

3.5.2.2 Reservoir Performance for Skin Magnitude of 6.4255

3.5.2.2.1 No Injection Well (No Pressure Maintenance)

At a formation damage magnitude of 6.4255, the reservoir is expected to perform poorly in terms of pressure predictions in the production grid for a non-pressure maintenance scenario as compared to a damage magnitude of 3.9255. Here, the reservoir can only produce for a maximum of 45 days with a corresponding pressure of 3821.98 psia as compared to a 61 day production period at 3825.86 psia for a damage magnitude of 3.9255.

As observed in Figure 14, the maximum predictable pressure for this case is 3747. 50 psia after about 9 months, for which is still lower than the saturation pressure. It is also expected that for this case, only a single-phase liquid is expected to constitute a bulk of the block saturation.

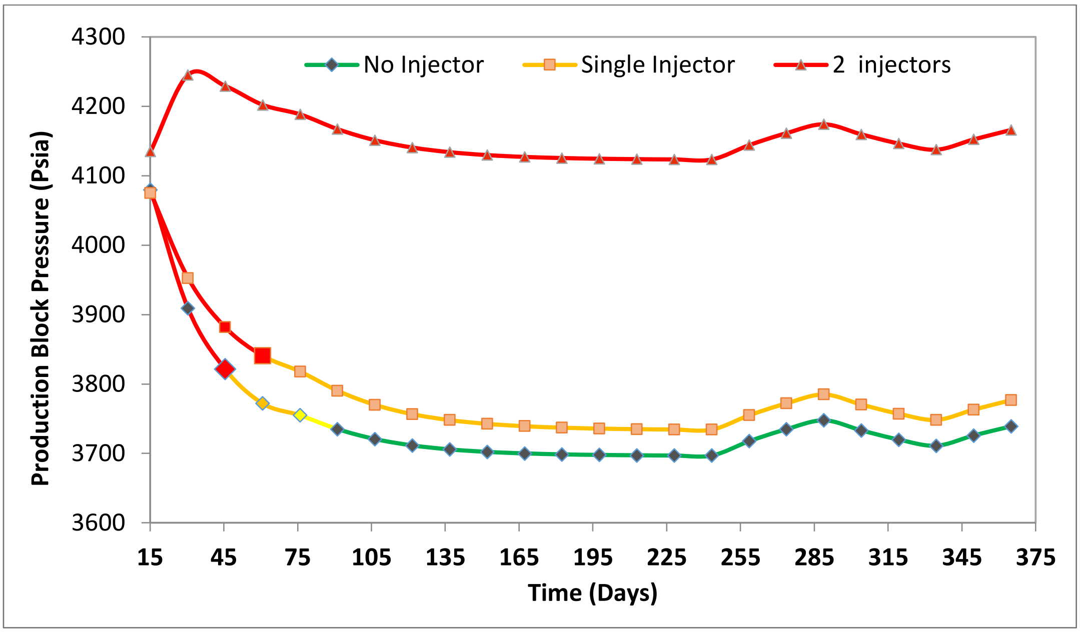

Figure 14: One Year Pressure Forecast for Production Well Grid at Skin Magnitude of 6.4255 for Different Pressure Maintenance Scenarios**.**

3.5.2.2.2 Pressure Maintenance Schemes

As observed in Figure 14, a single injector pressure maintenance scenario can only accommodate a single-phase gas saturation in the producing well block **4,4** for only about 2.5 months, after which the production well grid block pressure of 3817.84 psia will drop to below the dew point pressure to initiate the retrograde phenomenon before the next 15 days of production. This, to a large extent, tends to reveal the implication of increased formation damage in reservoir systems on the well productivity. A single injector pressure maintenance scheme could comfortably accommodate a single-phase production for a year at a formation damage magnitude of 3.9255. Here, only a maximum of 2.5 months for a damage magnitude of 6.4255 is predicted with both cases at the same injection rates and well locations.

The two – injector system still proved best as reservoir deliverability can comfortably maintain a single-phase underground gas withdrawal throughout a 1 year production period as shown in figure 14 above. The pressure forecast for the production grid records a minimum predictable pressure of the block after 243 days of production as 4123.36 psia. This 4123.36 psia pressure prediction, higher than the dew point pressure implies that regardless of the skin magnitude of 6.4255, there will be no chance of retrograde condensation phenomenon since the pressure is sufficiently maintained through the dual injectors.

3.5.2.3 Reservoir Performance for Skin Magnitude of 8.9255

Pressure forecast at higher skin ranges for the production block reveals that numbers of injectors notwithstanding, for a constant withdrawal rate of 55.00 MMscf of single-phase gas per day, production optimization at a skin magnitude of 8.9255 becomes a problem. As shown in Figure 15, single-phase gas distribution is impossible, even for the dual injection system. Production can only be accommodated for a maximum of 30 days, after which the pressure in the production well block drops below 3829.80 psia to begin the retrograde condensation phenomenon. After about 167 days, if the production well is still open to flow, the well block pressure response behaves as though there is no pressure maintenance scheme. For such cases, it is suggested that production is suspended for a while with the formation been hydraulically fractured to create artificial flow channels in zones of reduced permeability.

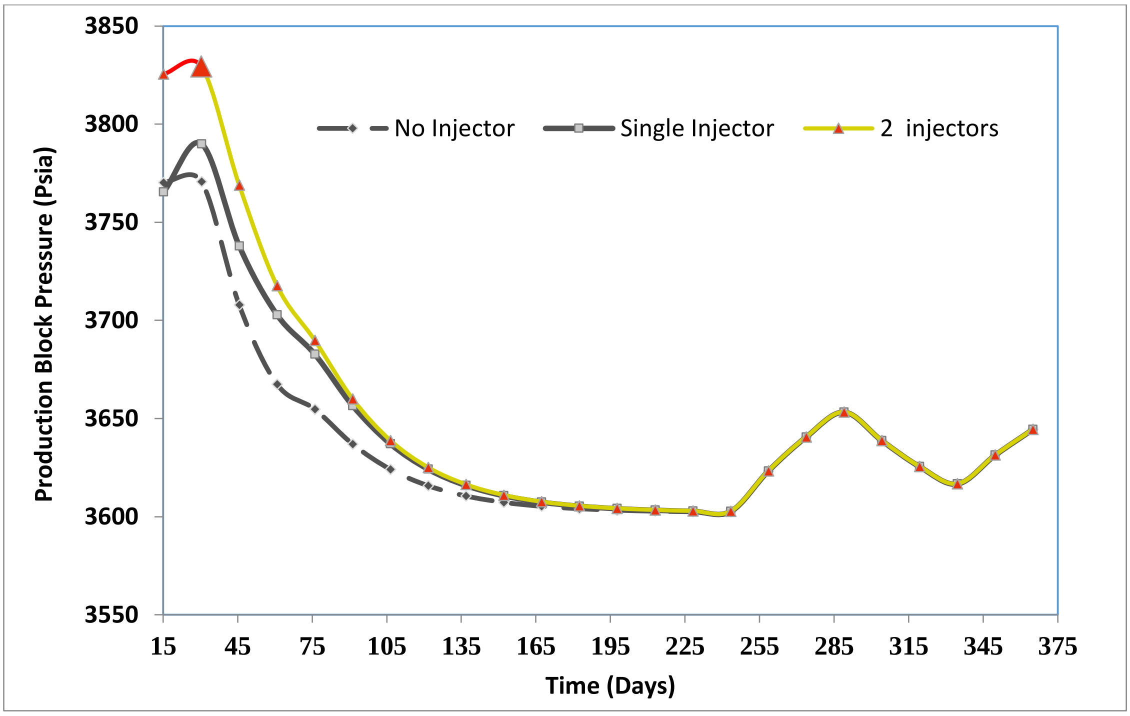

Figure 15: One Year Pressure Forecast for Production Well Grid at Damage Magnitude of 8.9255 for Different Pressure Maintenance Scenarios.

It is often advised after considering all intrinsic factors that producers must always operate within optimum production rates (Li *et al.*, 2019) For these unique reservoir systems, formation type, reservoir pressure, fluid saturation, rock and fluid properties, reservoir drive mechanism, and other dynamic parameters must be incorporated during reservoir pressure and well deliverability evaluations. Considering a loosely packed reservoir sand or an unconsolidated sandstone formation, prone to sanding problems during production, it is almost certain that skin effect or formation damage magnitude tends to increase as production continues. Additional pressure drops due to the effect of skin are usually of significant magnitudes and tend to hamper well productivity. The larger the magnitude of the formation damage, the higher the pressure drop around the wellbore vicinity which in turn reduces well deliverability. As observed for the above-mentioned skin scenario of magnitude 8.9255, if production is to be maintained at the rate of 55 MMscf/day, reservoir single-phase gas deliverability becomes a problem as the production well block becomes fully saturated with single-phase liquids (condensates).

3.6 Cumulative Material Balance Checks

To establish the validity of the solutions so presented in this study, the forecasted pressures are usually checked to ascertain if they satisfy material balance evaluations. This material balance concept usually accounting for mass conservation within a control volume (for which in this case, we consider a gas condensate reservoir) will to a laudable extent, inform the adaptability of the deduced solutions to other reservoir systems. This analysis simply involves taking the ratio of the accumulated mass to the net mass entering or leaving the gas condensate reservoir system.

In the figure below, a cumulative material balance for the 3.9255 skin magnitude evaluation is presented for the dual injector system. Since pressure is to be maintained to meet production constraints, mass or volumetric entry must to some extent, equate mass or volumetric exit. This is to say that the ratio of mass entry or volumetric entry into the system to that of the mass withdrawal or volumetric withdrawal must approximate to unity. From the C_{MB} – time plot, it is observed that pressure is sufficiently maintained to have yielded an average C_{MB} of 1.00001781 for the one year of investigation. The same can be computed for other skin magnitudes. It is important to note that C_{MB} must be in the range of 0.995 to 1.005 to achieve an acceptable solution (Eterkin *et al*., 2001).

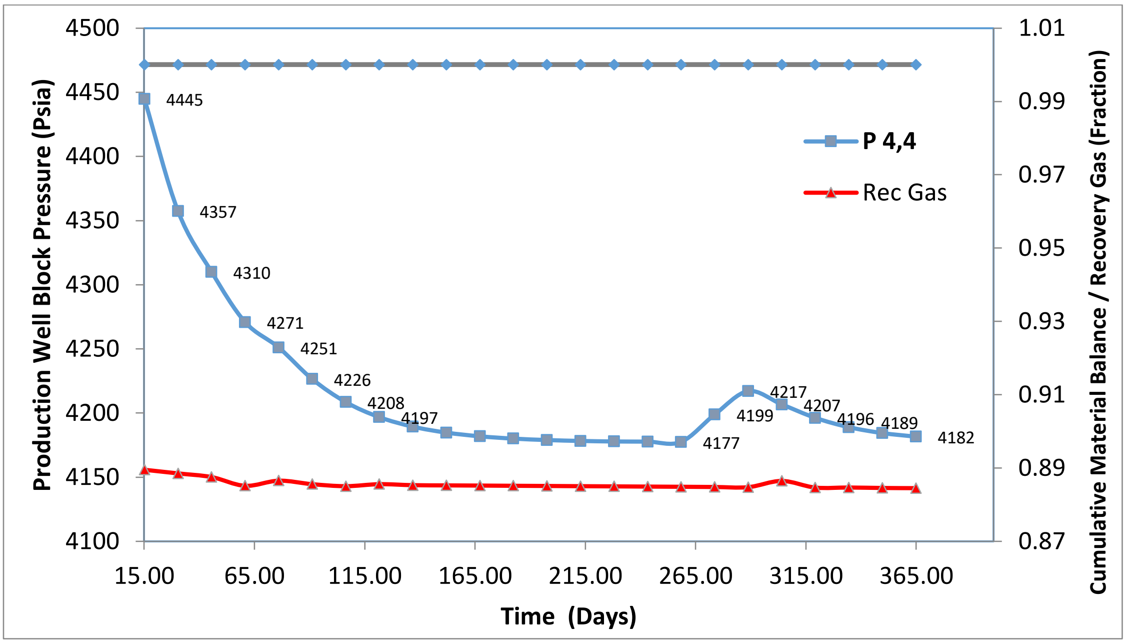

Figure 16: Variation in Production Block Pressure, Cumulative Material Balance and Recovery Gas Fraction with Time for Skin Magnitude of 3.9255

IV. CONCLUSION

The 3 – D model presented in this study has established a predictive and reservoir monitoring tool for qualitative evaluation and performance prediction for skin – prone Niger Delta sandstone gas condensate reservoirs. The model, in its 3 – D form, derived from the basic mass conservation expression can be adopted for these unconventional reservoirs provided accurate PVT model parameters are made available with sound PVT modeling procedure.

Considering some assumptions made during modeling processes (also considering initial reservoir conditions of temperature and pressure; fluid saturation; boundary conditions; the natural, physical and compositional properties of the reservoir), the 3D predictor model was reduced to accurately mimick the Niger Delta system. For example, assumptions such as the thin-bed nature of the reservoir with a net pay thickness of 103 ft as compared to its X – Y plane of 3,500 ft for each grid strongly influenced the decision of reducing the model from its 3D form to a 2 - dimensional analysis on an X and Y plane.

Also, with a sound and resolute theoretical background, the assumption of skin being most influential in the producing well block revealed that the production grid (**4,4**) is most prone to a Region–1 typed condensate saturation with effects slightly felt in neighboring blocks. Reason being that as production continues, regardless of pressure maintenance, fines and micro sandstone particles smaller than the pores of the reservoir system flow alongside the fluids. It is important to note that the pressure maintenance process via gas injection cannot retard skin effect but can only reduce to its barest minimum, the average maximum pressure drop of the system to maintain pressure above the dew point pressure of 3817.04 psi. Therefore, for a pressure-sensitive system such as gas condensate reservoirs, withdrawal rates must be optimal as it strongly influences the rate at which fines are transported and accumulated within the production well vicinity.

The model, so obtained from this work has provided a predictive tool for both the qualitative and quantitative analysis of reservoir flow dynamism in Niger Delta gas condensate fields.

The 3–Dimensional form of the model is not limited to Niger Delta reservoirs alone as it can serve accurately for all formation types, provided the relative permeability analysis which is a function of the wetting properties of the rock is conducted for that specific formation type.

Also, its findings have supported the re-evaluation of productivity enhancement techniques of already abandoned gas condensate fields due to condensate banking, as well as improving on other retrograde condensation mitigation techniques.

REFERENCES

Abekah, B. (2016). *Development of a Gas Condensate Reservoir: Case Study of the Niger Delta* (Master Thesis, Department of Petroleum Engineering, African University of Science and Technology).

Azamifard, A., Hekmatzadeh, M., & Dabir, B. (2016). Evaluation of Gas Condensate Reservoir Behavior using Velocity Dependent Relative Permeability during the Numerical Well Test Analysis. *Petroleum*, *2*(2), 156-165.

Bennion, D. B. (2003). *Improving well Productivity by Evaluating and Reducing Formation Damage during Overbalanced and Underbalanced Drilling Operations*. Ph.D. Thesis, University of Calgary.

Boe, A., Skjaeveland, S. M., & Whitson, C. H. (1989). Two-Phase Pressure Test Analysis. *SPE Formation Evaluation, 4* (04), 604-610.

Charlton, T. B., Kegg, S., Morgan, J. E., Zerpa, L. E., Koh, C. A., May, E. F., & Aman, Z. M. (2019). Application of a Transient Deposition Model for Hydrate Management in a Subsea Gas-Condensate Tieback. In *Offshore Technology Conference*. Offshore Technology Conference.

Coats, K. H. (1985). Simulation of Gas Condensate Reservoir Performance. *Journal of Petroleum Technology*, *37* (10), 1-870.

Dake, L. P. (2001). *The Practice of Reservoir Engineering (Revised Edition)* (Vol. 36). Elsevier.

Del Castillo Maravi, Y. (2004). *New inflow Performance Relationships for Gas Condensate Reservoirs* (Doctoral Dissertation, Texas A&M University).

Elsharkawy, A. M., Hashem, Y. S. K. S., & Alikhan, A. A. (2001). Compressibility Factor for Gas Condensates. *Energy & fuels*, *15* (4), 807-816.

Ertekin, T., Abou-Kassen, J. H., & King, G. R. (2001). *Basic Applied Reservoir Simulations*. Society of Petroleum Engineers. Richardson, Texas.

Fan, L., Harris, B. W., Jamaluddin, A., Kamath, J., Mott, R., Pope, G. A., & Whitson, C. H. (2005). Understanding gas-condensate reservoirs. *Oilfield Review*, *17* (4), 14-27.

Farid, A. M., El-Banbi, A., & Abdelwaly, A. A. (2013). An Integrated Model for History Matching and Predicting Reservoir Performance of Gas/Condensate Wells. *SPE Reservoir Evaluation & Engineering*, *16*(04), 412-422.

Fattah, K. A. (2012). A New Approach to Calculate Oil-Gas Ratio for Gas Condensate and Volatile Oil Reservoirs Using Genetic Programming. *Oil and Gas Business*, *1*, 311-323.

Fevang, O., & Whitson, C. H. (1996). Modeling Gas-condensate Well Deliverability. *SPE Reservoir Engineering*, 11 (4), 221-230.

Fussell, D. D. (1973). Single-Well performance predictions for Gas Condensate Reservoirs. *Journal of Petroleum Technology*, 25 (7), 860-870.

Gundersen, P. L. (2013). *Compositional Simulations of Producing Oil-Gas Ratio Behaviour in low Permeable Gas Condensate Reservoir* (Master's Thesis; University of Stavanger, Norway).

Hajizadeh Mobaraki, A., Bashir, A., Shen Sow, C., Deo Tewari, R., & BM Zakei, A. (2019). Integrated Approach for Proper Resource Assessment of a Challenging Over-Pressured Gas Condensate Reservoir: Case Study of Analytical and Numerical Modeling of a Central Luconia Carbonate Field. In *SPE Oil and Gas India Conference and Exhibition*. Society of Petroleum Engineers.

Hashemi, A., Nicolas, L., & Gringarten, A. C. (2006). Well Test Analysis of Horizontal Wells in Gas-condensate Reservoirs. *SPE Reservoir Evaluation & Engineering*, *9*(01), 86-99.

Hou, D., Xiao, Y., Pan, Y., Sun, L., & Li, K. (2016). Experiment and Simulation Study on the Special Phase Behavior of Huachang Near-Critical Condensate Gas Reservoir Fluid. *Journal of Chemistry*, 23 (2), 77 – 92.

Ibeh, S. U., & Chubueze, S. E. (2016). PVT Analysis: Validity Checks and EOS Tuning Techniques for Retrograde Gas Condensate Reservoirs. In *SPE Nigeria Annual International Conference and Exhibition*. Society of Petroleum Engineers.

Ikoku, C (1992). *Natural gas Production Engineering*. Krieger Publishing Company. Malabar, Florida, USA.

Ikoku, C (1992). *Natural gas Reservoir Engineering*. Krieger Publishing Company. Malabar, Florida, USA.

Izuwa, N. C., & Nwosu, C. N. (2014, August). Influence of Aquifer Support on Gas Condensate Reservoir Performance. In *SPE Nigeria Annual International Conference and Exhibition*. Society of Petroleum Engineers.

Kabir, A., Ahmed, M., & Elew, D. (2019). Three Dimensional Compositional Variation in Gas Condensate Reservoirs. In *SPE Middle East Oil and Gas Show and Conference*. Society of Petroleum Engineers.

Khanal, A. (2014). *Effect of Reservoir and Completion Parameters on Production Performance in Gas Condensate Reservoirs* (Doctoral Dissertation, University of Houston, Texas).

Lal, R. R. (2003). *Well Testing in Gas-Condensate Reservoirs* (Doctoral dissertation, Stanford University).

Li, G., Guo, B., Li, J., & Wang, M. (2019). A Mathematical Model for Predicting Long-Term Productivity of Modern Multifractured Shale-Gas/Oil Wells. *SPE Drilling & Completion*.

Li, K., & Firoozabadi, A. (2000). Phenomenological Modeling of Critical Condensate Saturation and Relative Permeabilities in Gas/Condensate Systems. *SPE Journal*, *5* (02), 138-147.

Li, Z., & Firoozabadi, A. (2012). General Strategy for Stability Testing and Phase-Split Calculation in Two and Three Phases. *SPE Journal*, *17*(04), 1-096.

Mansoori, G. A. (2009). A Unified Perspective on the Phase Behavior of Petroleum Fluids. *International Journal of Oil, Gas and Coal Technology*, *2* (2), 141-167.

Mazloom, J., & Rashidi, F. (2006). Use of Two-Phase Pseudo Pressure Method to Calculate Condensate Bank Size and Well Deliverability in Gas Condensate Reservoirs. *Petroleum science and technology*, *24* (2), 145-156.

McCain Jr, W. D. (1994). Heavy Components Control Reservoir fluid Behavior. *Journal of Petroleum Technology*, *46* (09), 746-750.

Medina Tarrazzi, T. M. (2003). *Characterization of gas condensate reservoirs using pressure transient and production data-Santa Barbara Field, Monagas, Venezuela* (Doctoral dissertation, Texas A&M University, Texas).

Mindek, C. (2005). *Production Optimization of a Gas Condensate Reservoir using a Black oil Simulator and Nodal System Analysis: A Case Study* (Doctoral Dissertation, Middle East Technical University).

Montazeri, G. H., Dastkhan, Z., & Aliabadi, H. (2011). Effect of Relative Permeability on Well testing Behavior of Naturally Fractured lean Gas Condensate Reservoirs. *World Academy of Science, Engineering and Technology, International Journal of Chemical, Molecular, Nuclear, Materials, and Metallurgical Engineering*, *5*(6), 460-464.

Mott, R. (2003). Engineering Calculations of Gas-Condensate-Well Productivity. *SPE Reservoir Evaluation & Engineering*, *6* (05), 298-306.

Niemtschik, G. E., Poettmann, F. H., & Thompson, R. S. (1994). Gas-Condensate Composition--1: New Correlation Determines Retrograde Gas-Condensate Composition. *United States Oil and Gas Journal;* 92 (44).

Orodu, O. D., Ako, C. T., Makinde, F. A., & Owarume, M. O. (2012). Well Deliverability Predictions of Gas Flow in Gas-Condensate Reservoirs, Modelling Near-Critical Wellbore Problem of Two-Phase Flow in 1-Dimension. *Brazilian Journal of Petroleum and Gas*, *6* (4).

Pope, G. A., Wu, W., Narayanaswamy, G., Delshad, M., Sharma, M. M., & Wang, P. (2000). Modeling Relative Permeability Effects in Gas-Condensate Reservoirs with a New Trapping Model. *SPE Reservoir Evaluation & Engineering*, *3* (02), 171-178.

Raghavan, R., & Jones, J. R. (1996). Depletion Performance of Gas-Condensate Reservoirs. *Journal of Petroleum Technology*, *48* (08), 725-731.

Roussennac, B. (2001). *Gas Condensate Well Test Analysis* (Doctoral dissertation, Stanford University).

Safari-Beidokhti, M., & Hashemi, A. (2016). Condensate Blockage Effects in Well Test Analysis of Dual-Porosity/Dual-Permeability, Naturally Fractured Gas Condensate Reservoirs: a Simulation Approach. *Journal of Petroleum Exploration and Production Technology*, *6*(4), 729-742.

Saradva, H., Jain, S., Hamadi, M. A., Thakur, K. K., Govindan, G., & Ahmed, A. F. M. (2019). Evaluating Liquid Loading Using Multiphase Dynamic Flow Simulation in Complex Openhole Multilateral Gas Condensate Wells. In *SPE Middle East Oil and Gas Show and Conference*. Society of Petroleum Engineers.

Sarvestani, M. T., Rashidi, F., & Dehghani, S. A. M. (2016). A Production Data Analysis Model for Gas/Condensate Reservoirs. *Journal of Petroleum Science and Engineering*, *141*, 52-69.

Sen, N., & Nwabia, F. N. (2017). Validation of an Estimated Gas Condensate Reserve using Applied Uncertainty Analysis for the Condensate Reservoir Properties. *International Journal of Engineering Works*, *4* (1), 21-28.

Siddiqui, M. A., Tariq, S. M., Haneef, J., Ali, S. I., & Manzoor, A. A. (2019). Asphaltene Stability Analysis for Crude Oils and Their Relationship With Asphaltene Precipitation

Models for a Gas Condensate Field. In *SPE Middle East Oil and Gas Show and Conference*. Society of Petroleum Engineers.

Singh, K., & Whitson, C. H. (2010). Gas-Condensate Pseudo-pressure in Layered Reservoirs. *SPE Reservoir Evaluation & Engineering*, *13* (02), 203-213.

Skuzovatov, M. Y. (2017). Natural Gas and Condensate Reserves in the Angara-Lena Gas-bearing region. *Russian Geology and Geophysics*, *58*(3), 503-515.

Tarek A. (2006). Reservoir Engineering Handbook. Elsevier: Gulf Professional Publishing. Third Edition.

Terry, R. E., Rogers, J. B., & Craft, B. C. (2013). *Applied petroleum reservoir engineering*. Pearson Education.

The World Factbook (2017, January 1). https://www.cia.gov/library/publications/the-world-factbook/fields/2253.html#ni Central Intelligence Agency.

Tompkins, M. W., Ebbs, D. J., Thomas, L. K., & Dixon, T. N. (1993). Chatom Gas Condensate Cycling Project. *SPE Advanced Technology Series*, *1* (02), 152-160.

Vo, H. X., & Roland, N. (2011). Composition Variation during Flow of Gas-Condensate Wells Project Number 07122-29. FINAL.

Wall, C. G. (1982). Characteristics of Gas Condensate Reservoirs and Traditional Production Methods. *North Sea Gas Condensate Reservoirs and their Development 1982*, 1-12.

Whitson, C. H., Fevang, O & Yang, T. (1999). Gas Condensate PVT–What's Really Important and Why?. In *IBC Conference on Optimization of Gas Condensate Fields*, London.

Wilson, B. W. (2004). *Modeling of Performance Behavior in Gas Condensate Reservoirs using a Variable Mobility Concept* (Doctoral Dissertation, Texas A&M University).

Wu, Y., Cheng, L., Huang, S., Fang, S., Killough, J. E., Jia, P., & Wang, S. (2019). A Transient Two-Phase Flow Model for Production Prediction of Tight Gas Wells with Fracturing Fluid-Induced Formation Damage. In *SPE Western Regional Meeting*. Society of Petroleum Engineers.

Zendehboudi, S., Ahmadi, M. A., James, L., & Chatzis, I. (2012). Prediction of condensate-to-gas ratio for retrograde gas condensate reservoirs using artificial neural network with particle swarm optimization. *Energy & Fuels*, *26*(6), 3432-3447.